THERMODYNAMIC PROPERTIES OF ARGON GAS IN THE TEMPERATURE-RANGE 100-3000 K

Amal F. Al-Maaitah
Department of Physics, Mu'tah University, Al-Karak, Jordan
E-mail:amal.almaaitah@yahoo.com

ABSTRACT: *In this paper, the classical second virial coefficient and the corresponding first quantum correction for Ar gas are calculated in the temperature range 100-3000 K. These calculations are based on the Ar-Ar interaction potential. The Boyle and Joule inversion temperatures are determined. The thermodynamic properties of the system are calculated. These comprise the equation of state (pressure-density-temperature relations), total internal energy, entropy and Helmholtz free energy. The compressibility Z is evaluated as a measure of non-ideality of the gas. The deviation from ideality becomes most significant at low temperatures.*

Keywords: The Second virial coefficient; Argon; Boyle's temperature; Equation of state.

1. INTRODUCTION

This work addresses both the classical second virial coefficient B_{cl} and the corresponding quantum correction B_{qc} in the temperature-range 100-3000 K. This coefficient is important in its own right. For one thing, it provides valuable information about the intermolecular forces. For another, B helps to obtain the Boyle's temperature in which the attractive and repulsive interactions balance. At low densities, the deviation from the ideal state is measured by the second virial coefficient [1]. This coefficient can be used as a predictor of the borderline between the classical and quantum regimes in a nonideal gas [2]. Also, It is used as a starting point for determining the thermophysical properties of real gases.

Many theoretical methods were developed to investigate the properties of Ar gas. An *ab initio* potential was used to calculate thermophysical properties of argon phases [3]. Monte Carlo simulations were used to predict the thermophysical properties of pure Ar as well as the binary mixtures Ne-Ar [4]. A statistical-mechanical perturbation theory was used to derive an analytic equation of state. This equation was applied to calculate the thermodynamic properties, including the vapor pressure curve, compressibility factor, fugacity coefficient [5], internal energy, enthalpy, entropy and heat capacity [6], using the Lennard-Jones 12-6 potential.

The main input in calculating B_{cl} and B_{qc} is the interaction potential. In this paper, the HFD-B3 potential is used; this is generally consists of a strongly-repulsive short-range part, a weakly-attractive long-range part and a minimum in between representing the equilibrium configuration for the interacting pair [7].

2. Formalism

2.1 The Second Vrial Coefficient

B_{cl} and the corresponding B_{qc} are given by [8]

$$B_{cl}(T) = 2\pi\int_0^\infty \left[1 - e^{-\beta V(r)}\right] r^2 dr \; ; \qquad (1)$$

$$B_{qc}(T) = \frac{\pi\hbar^2\beta^3}{6m}\int_0^\infty \left[e^{-\beta V(r)}\right]\left(V'(r)\right)^2 r^2 dr \; , \qquad (2)$$

where V(r) is the binary interatomic potential, V′(r) is its first derivative with respect to the argument r, which is the magnitude of the interatomic separation, and β is the temperature parameter $(k_B\ T)^{-1}$, k_B being Boltzmann's constant.

The input potential is chosen as the HFD-B3 for Ar-Ar interactions. The HFD-B3 potential V(r) is plotted in Figure 1 and is given by

$$V(r) = \varepsilon V^*(x) \qquad (3)$$

$$V^*(x) = A\exp\left(-\alpha x + \beta x^2\right) - \left\{\frac{C_6}{x^6} + \frac{C_8}{x^8} + \frac{C_{10}}{x^{10}}\right\}F(x)$$

(4)

$$F(x) = \begin{cases} \exp\left[-\left\{\frac{D}{x} - 1\right\}^2\right], & x < D \\ 1, & x \geq D \end{cases} \qquad (5)$$

$$x \equiv \frac{r}{r_m}$$

The parameters for Ar-Ar potential are tabulated in Table 1.

Table 1: Parameters for Ar-Ar potential.

Parameters	HFD-B3
A	1.13211845×10^5
r_m	3.761Å
ε	143.25 K
D	1.04
α	9.00053441
β	-2.60270226
C_6	1.09971113
C_8	0.54511632
C_{10}	0.39278653

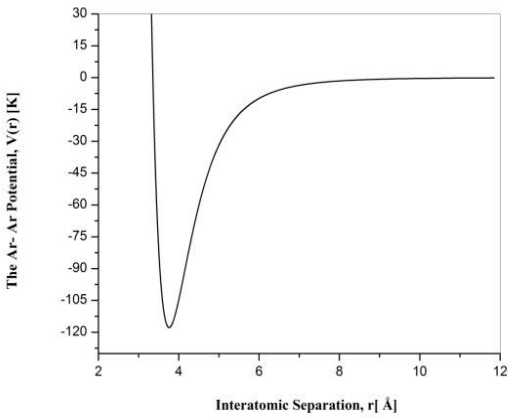

Fig. 1: The Ar- Ar potential, V(r), as a function of the interatomic separation r.

2.2 Thermodynamic Properties

The thermodynamic properties in the gas phase are defined as follows:

a) The pressure P, which can be calculated from the virial equation of state [9]

$$\frac{P}{nk_BT} = 1 + nB \qquad (6)$$

b) The compressibility factor Z, which measures the non-ideality of the gas. This is given by [10]

$$Z = 1 + nB. \qquad (7)$$

For an ideal gas, Z=1, since PV= Nk_BT; n ≡ N/V (B = 0).

c) The Helmholtz free energy F (N, V, T), which is given by [11]

$$F = Nk_BT\left(\ln\left(n\lambda^3\right) - 1 + B(T)n\right). \qquad (8)$$

d) The entropy S,which is an expression of the disorder, or randomness of a system. It is defined at a constant volume as [12]

$$S = -\left(\frac{\partial F}{\partial T}\right)_V. \qquad (9)$$

e) The total internal energy U, includes potential and kinetic energy. It depends on the density and temperature of the gas and is given by [13]

$$U = Nk_BT\left(1.5 - nT\frac{dB}{dT}\right). \qquad (10)$$

3. RESULTS AND DISCUSSION

3.1 The Second Virial Coefficient

The variation of B_{cl} with T is shown in Figure 2, and in Table 2. The corresponding variation for B_{qc} with T is shown in Table 2. In the low T-limit, where the attractive part of the interaction potential for argon atoms dominates, B_{cl} is large and negative. It increases as T increases, becoming less negative. At a certain temperature, Boyle's temperature T_B, B_{cl} has zero value, where the attractive and repulsive interactions balance. $T_B \approx 411.003$ K. Thereafter, B_{cl} becomes positive. This is because the interaction is dominated by the repulsive part. By increasing T, B increases until it reaches a maximum value at inversion temperature T_i after which it decreases. The maximum value of B_{cl} occurs at $T_i \approx 2556$ K which is in the range ($T_i \approx 3800 \pm 1800$ K) reported by Boschi-Filho and Buthers [14].

On the other hand, B_{qc} decreases with increasing T, as shown in Table 2. The ratio$|B_{qc}|/|B_{cl}|$ indicates that $|B_{qc}|$ is less than $|B_{cl}|$; B_{cl} dominates with increasing T. This means that quantum character disappear gradually with increasing temperature.

The calculated values of classical second virial coefficient are compared to previous theoretical [1, 15] as well as experimental [16, 17] results in Tables 3 and 4; respectively. T_B is given in Table 5, together with the previous results. Clearly, the present results are comparable to the previous results

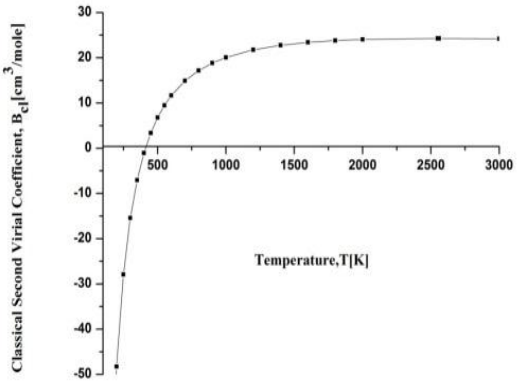

Fig. 2: B_{cl} [cm^3/mole] versus the temperature T [K].

Table 2: The variation of B_{cl} together with the corresponding B_{qc} with temperatures.

T [K]	B_{cl} [cm^3/mole]	B_{qc} [cm^3/mole]
100	-183.91	48.348
150	-86.741	16.526
200	-48.29	8.640
250	-27.94	5.485
300	-15.45	3.882
350	-7.06	2.940
400	-1.09	2.334
450	3.36	1.915
500	6.78	1.612
550	9.47	1.384
600	11.64	1.207
700	14.88	0.952
800	17.16	0.779
900	18.82	0.655
1000	20.06	0.562
1200	21.74	0.432
1400	22.76	0.348
1600	23.40	0.289
1800	23.80	0.245

2000	24.05	0.212
2400	24.20	0.165
2550	24.25	0.153
2556	24.26	0.152
2560	24.24	0.152
3000	24.18	0.123

Table 3: Comparison of computed B_{cl} with some previous theroretical results at different temperatures.

T	B_{cl} [This work]	$B_{cl)th}$ [1]	$B_{cl)th}$ [15]
100	-183.91		-184.11
200	-48.29		-48.363
300	-15.45		-15.452
400	-1.09	-1.02	-1.0546
500	6.78	7.02	6.8385
600	11.64	12.06	
700	14.88	15.46	
800	17.16	17.86	
900	18.82	19.64	
1000	20.06	20.98	
1200	21.74	22.84	
1400	22.76	24.01	
1600	23.40	24.79	
1800	23.80	25.30	
2000	24.05	25.65	
2400	24.20	26.04	

Table 4: Comparison of computed B_{cl} with some previous experimental results at different temperatures .

T	B_{cl} [This work]	B_{exp} [16]	B_{exp} [17]
100	-183.91		-185.50
200	-48.29		-47.60
300	-15.45		-15.60
400	-1.09	-0.82	-0.90
500	6.78	7.17	7.30
600	11.64	12.25	
700	14.88	15.67	
800	17.16	18.09	
900	18.82	19.84	
1000	20.06	21.19	
1200	21.74	23.01	
1400	22.76	24.03	
1600	23.40	24.86	
1800	23.80	25.49	
2000	24.05	25.91	
2400	24.20	26.24	

Table 5: The Boyle temperature T_B [K] for the HFD-B3 potential compared with previous results.

T_B [This work]	T_B [1]	T_B [18]	T_B [19]	T_B [20]
411.003	410.151	407.76	407.59	408.35

3.2 Thermodynamic Properties

In Figure 3, the compressibility Z is plotted versus the temperatures T. It is observed that at low temperatures (T<400 K), Z of argon gas increases by increasing T. For Z < 1, attractive forces dominate and the volume of the gas is less than that predicted by the ideal-gas equation of state. The nonideality decreases gradually with increasing T. It is evident that the system exhibits as an ideal gas at high temperature.

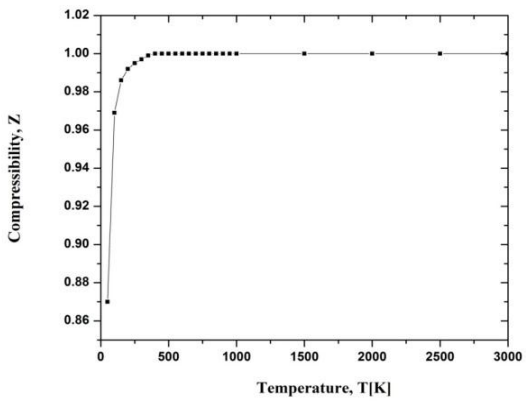

Fig. 3: The compressibility Z versus the temperatures T [K].

Figure 4 displays the pressure P versus the temperature T. It is shown that P increases with increasing T. The P-T curves represents the equation of state of the system.

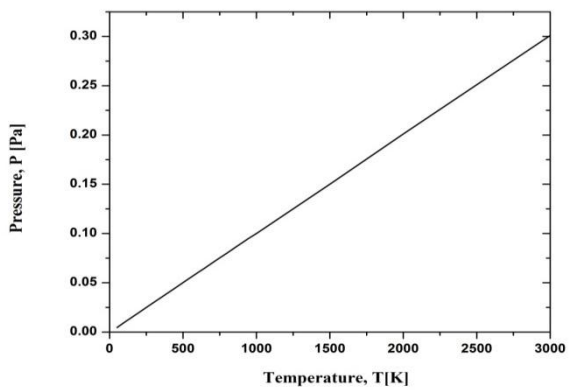

Fig. 4: The pressure P [Pa] versus the temperature T [K].

In Figure 5, The Helmholtz free energy F is plotted as a function of T. It is shown that F decreases as T increases.The Helmholtz free energy tends to minimize as the system tends to equilibrium state in which the entropy has the highest possible value.

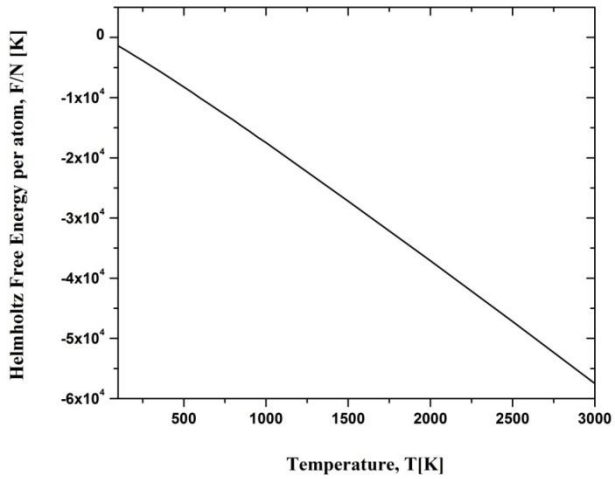

Fig. 5: The Helmholtz free energy F/N [K] versus temperature T [K].

Figure 6 displays the entropy S versus the temperature T. It is shown that S increases with increasing T.

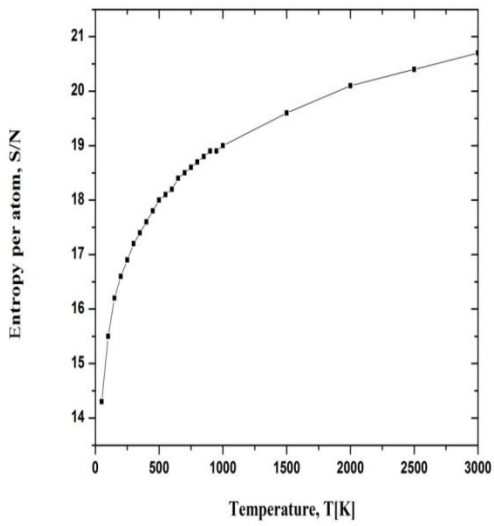

Figure 6: The entropy per atom S/N versus temperature T [K].

Figure 7 shows the internal energy U versus the temperature T. It is shown that U increases with increasing T since the repulsive forces increase.

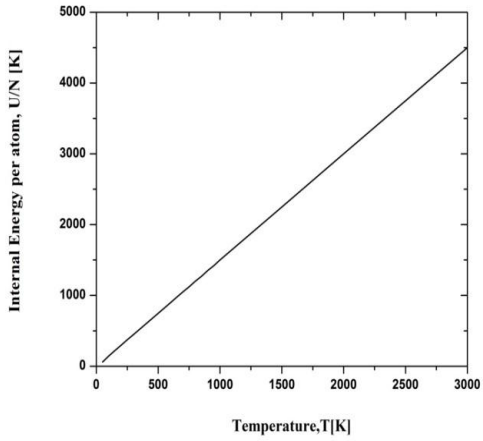

Fig. 7: The total internal energy U/N [K] versus the temperature T [K]

4. CONCLUSION

In this paper, extensive results for thermodynamic properties of Ar gas are presented in the temperature-range 100-3000K. The classical second virial coefficient and the corresponding first quantum correction are calculated. These calculations are all undertaken using the HFD-B3 potential as a main input. The thermodynamic properties of the gas – the compressibility, pressure-density-temperature behavior, Hemholtz free energy and total internal energy- are then readily followed. Also, the Boyle and Joule inversion temperatures are determined. The deviation from ideality becomes most significant at low temperatures. There is a good agreement with previous results.

REFERENCES

[1] A. Hutem, S. Boonchui (2012), Numerical evaluation of second and third virial coefficients of some inert gases via classical cluster expansion, *J Math Chem*, 50:1262–1276.

[2] H.B. Ghassib, A.S. Sandouqa, B.R. Joudeh, S.M. Mosameh (2014), Predicting the borderline between the classical and quantum regimes in 4He gas from the second virial coefficient, *Can. J. Phys*. 92 ,997.

[3] A.E. Nasrabad, R. Laghaei (2006), Computational Studies on Thermodynamic Properties, Effective Diameters, and Free Volume of Argon Using *ab initio* Potential, *J. Chem. Phys*. 125, 084510.

[4] A.E. Nasrabad, R. Laghaei, U.K. Deiters (2004), Prediction of the Thermophysica Properties of Pure Neon, Pure Argon, and the Binary Mixtures Neon-Argon and Argon-Krypton by Monte Carlo Simulation Using ab initio Potential, *J. Chem. Phys*. 121, 6423.

[5] F. Mozaffari (2011), An Equation of State for Argon, *J. Phys. Chem*. Electrochem. 2, 2109.

[6] F. Mozaffari, Z.Z. Sharabadi (2011), Thermodynamic Properties for Argon, *J. Phys. Chem. Electrochem.*1, 139.

[7] R.A. Aziz, M.J. Slaman (1990), The repulsive wall of the Ar–Ar interatomic potential reexamined, *J. Chem. Phys.* 92, 1030.

[8] A. A. Al Ajaleen, A.S. Sandouqa, and H.B. Ghassib (2019), The second virial coefficient for Rubidium-87 (^{87}Rb) gas in the temperature-range 1000-40000 K and beyond, *British Journal of Science*, Vol. 17 (1).

[9] R. P. Feynman (1992), Statistical Mechanics: A Set of Lectures (Benjamin, Reading, MA).

[10] S. M. Mosameh, A. S. Sandouqa, H. B. Ghassib and B. R. Joudeh (2014), Thermodynamic Properties of 4He Gas in the Temperature Range 4.2-10 K, *J. Low Temp. Phys*. 175, 523.

[11] B. A. Mamedov and E. Somuncu (2017). Accurate Evaluation of the Internal Energy, Free Energy, Entropy and Enthalpy of Non-Polar Molecules by Using Virial Coefficients. *Chinese Journal of Physics*, 000, 1-16.

[12] F. Reif (1965), Fundamentals of Thermal Physics. New York: McGraw-Hill.

[13] R. K. Patheria, P. D. Beale, (2011), Statistical Mechanics, Burlington, MA 01803.

[14] H. Boschi-Filho, and C. C. Buthers, Second virial coefficient for real gases at high temperature, eprint arXiv:cond-mat/9701185 v2 28, Jan 1997. [Online]. Available: http://arxiv.org/PS_cache/cond-mat/pdf/9701/9701185v2. pdf [Accessed March 15, 2009].

.

[15] Dias da Silva CJ, Brandão J, Varandas AJC (1989), Accurate diatomic curves for Ne_2, Ar_2, Kr_2 and Xe_2 form the extended Hartree–Fock approximate correlation energy model, *J. Chem. Soc*., Faraday Trans. 2, 85:1851

[16] J.H. Dymond, E.B. Smith (1980), The Virial Coefficients of Pure Gases and Mixtures: A Critical Compilation. Clarendon, Oxford

[17] J.H. Dymond, E.B. Smith (1969), The virial coefficients of gases: A critical compilation. Clarendon, Oxford

[18] Ch. Tegeler, R. Span, W. Wagner (1999), A New Equation of State for Argon Covering the Fluid Region for Temperatures From the Melting Line to 700 K at Pressures up to 1000 MPa, *J. Phys. Chem. Ref. Data* 28 779–850.

[19] R. Span, W. Wagner (2003), Equations of State for Technical Applications. I. Simultaneously Optimized Functional Forms for Nonpolar and Polar Fluids, *Int. J. Thermophys*. 24 41–109.

[20] R.B. Stewart, R.T. Jacobsen (1989), Thermodynamic properties of argon from the triple point to 1200 K at pressures to 1000 MPa, *J. Phys. Chem. Ref. Data* 18 639–798